(Received 21 January 2025, Accepted 17 June 2025, Scheduled 29 June 2025)

Design and Integration of a Flexible RFID UHF Antenna with a 3D Printed Fluid Channel for Liquids Sensing Applications

Mohammed A. Ennasar[1, *], Mohamed Elkhamlichi[1], Youness Akazzim[2], Abdelmounaim Tachrifat[1], Mariem Aznabet[1], Otman El Mrabet[1], and Mohsine Khalladi[1]

[1] *Intelligent System Design Laboratory (ISD), Faculty of Sciences, Abdelmalek Essaadi University, Tétouan 93000, Morocco*
[2] *Department of Signal Theory and Communications, Technical University of Catalonia, Barcelona 08034, Spain*

ABSTRACT: This article presents an innovative UHF RFID tag sensor featuring a flexible ring resonator dipole integrated with a fluidic channel. Leveraging the unique characteristics of the resonator dipole, the sensor demonstrates high sensitivity in detecting the dielectric properties of various liquids. The RFID integration facilitates wireless communication and remote monitoring, enabling real-time, continuous measurement of sensor data. The proposed RFID sensor design allows for easy attachment on the PLA fluid channel, enhancing its practical utility. Experimental results show a strong correlation with reference measurements obtained with traditional laboratory methods using VNA. The sensor achieves effective impedance matching up to 1 GHz, even without the presence of a liquid in the channel. Moreover, confining liquids with high dielectric constants within the channel broadens the operational range across the UHF RFID band, spanning 865 MHz to 928 MHz, and the wireless RFID tag sensor is well suited for applications requiring real-time analysis and continuous monitoring. The proposed flexible ring resonator dipole UHF RFID tag sensor, coupled with fluidic channel-based tuning, offers significant potential for applications such as chemical analysis of liquids. Its unique blend of flexibility, wireless data communication, and accurate dielectric characterization opens new avenues for noninvasive and remote sensing in liquid-based system.

1. INTRODUCTION

The growing interest in flexible electronics and the Internet of Things (IoT) has spurred the development of innovative, miniaturized sensors that are both portable and adaptable to various environments [1]. Among them, Radio Frequency Identification (RFID) technology has gained attention due to its wireless communication capabilities, ease of integration, and potential for passive operation without the need for an internal power source [2, 3]. RFID-based sensors, particularly those operating in the Ultra High Frequency (UHF) range, offer significant advantages for remote sensing applications, including long read ranges and the ability to embed sensors into flexible substrates.

Accurate detection of liquid solutions, such as sugar, ethanol, and acetic acid, is an important area of research. Several methods have been developed for measuring the concentration of aqueous liquids, with recent focus shifting toward RF and microwave sensors due to their advantages over traditional techniques. For instance, Wiltshire et al. [5] introduced a passive split-ring resonator tag configuration for RFID-based wireless permittivity sensing, while Vélez et al. [6] developed highly sensitive microwave sensors using open complementary split-ring resonators (OCSRRs) for dielectric characterization and solute concentration measurement in liquids. Additionally, Seo et al. [7] proposed a microfluidic eighth-mode substrate-integrated waveguide (EMSIW) antenna for compact ethanol chemical sensing. However, except for the work developed in [4], most of these methods rely on expensive equipment such as network analyzers and require specialized training, making them costly, complex, time-consuming, and dependent on direct contact with the liquid or large sample volumes. Therefore, there is a pressing need for new techniques that are cost-effective, rapid, contactless, and well suited for lab-on-chip applications.

Several studies have demonstrated the effectiveness of RFID tag antennas for liquid detection. For instance, a flexible tag antenna-based sensor for detecting NaCl and sugar in water was proposed in [4]. In [8], an RFID-based sensor was used to detect different types of liquids by observing the shift in resonant frequency, while [9] explored the use of a fluidic channel integrated with an RFID tag antenna for precise measurement of liquid permittivity. These advancements underscore the potential of RFID tag antennas as versatile and efficient tools for liquid sensing, offering a combination of flexibility, sensitivity, and wireless communication capabilities that are unmatched by traditional sensing methods [10, 11].

Flexible RFID tag antennas, fabricated using materials such as conductive inks on polymer substrates, offer additional advantages for liquid sensing. Their flexibility allows them to conform to various surfaces, including curved or irregular objects, making them suitable for integration into wearable devices or for embedding in non-planar structures [12, 13]. This adaptability, combined with the wireless communication capabilities of RFID technology, enables real-time and remote monitoring of liquids in diverse environments, ranging from industrial processes to healthcare applications [14]. Moreover, the

* Corresponding author: Mohammed Ali Ennasar (ennasar.moham-medali@gmail.com).

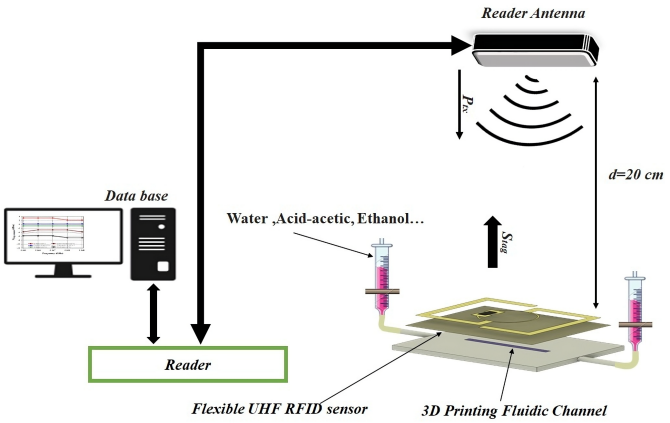

FIGURE 1. Schematic diagram of the wireless sensor system for liquid detection.

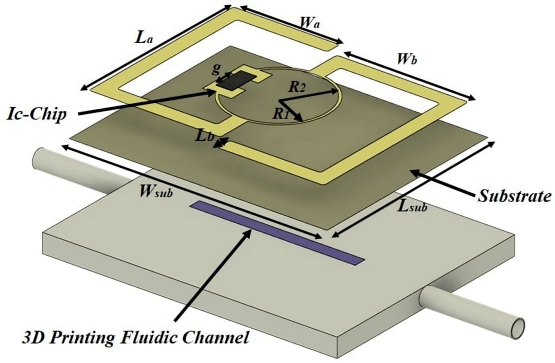

FIGURE 2. Configuration of the RFID tag sensor.

integration of RFID tag antennas with microfluidic or fluidic systems presents a powerful approach to enhancing liquid detection sensitivity and selectivity. Microfluidic channels can precisely control the flow of liquids over the RFID antenna, ensuring consistent interaction and improving the accuracy of the dielectric characterization [15]. This integration allows for miniaturized, portable, and cost-effective sensors that can be used in various applications, including environmental monitoring, chemical processing, and bioanalytical diagnostics [16].

In this work, we present a new method for characterizing liquid dielectrics using a flexible polymer ring resonator dipole UHF RFID tag sensor. This sensor has a built-in 3D fluid channel that allows the fluid to interact directly with the resonant structure. The design enables real-time monitoring of the fluid dielectric properties by exploiting the high sensitivity of ring resonators to changes in the surrounding dielectric environment. We discuss the design, fabrication, and experimental testing of the sensor and highlight its ability to effectively characterize various liquid dielectrics. The results show that the sensor can provide accurate, efficient, and wireless measurements, making it a promising option for applications that require portable and flexible sensing solutions.

2. RFID TAG SENSOR DESIGN AND METHODOLOGY

The proposed sensor system is depicted in Figure 1. It consists of an RFID tag sensor integrating a fluidic channel, an RFID reader, and a laptop for data processing. The fluidic channel is positioned beneath the gap where the RFID chip is located, to ensure greater interaction between the liquid and the RFID tag antenna, as shown in Figure 2.

Figure 1 shows a wireless liquid detection system that utilizes a flexible UHF RFID sensor embedded in a 3D printed liquid channel. This system is designed for the detection and analysis of various liquids such as water, acetic acid and ethanol. The flexible RFID sensor positioned in a Polylactic Acid (PLA) 3D printed channel interacts with the flowing fluids and allows the detection of their properties based on changes in the dielectric properties of the fluid. A reading antenna located 20 cm from the sensor sends radio frequency (RF) signals to the RFID sensor, which responds by modulating the signal according to the specific liquid it encounters. The reader then captures this modulated signal, which reflects the unique properties of the liquid. This information is then transmitted via the reader to a connected database, where the data is stored and analyzed over time. The system is an advanced and precise remote fluid detection platform that combines the versatility of RFID technology with the customizability of 3D printed fluid channels. It provides a flexible solution for monitoring and analyzing liquids composition in a wide range of applications, including industrial processes and laboratory research. The ability to store and analyze data over time makes it a valuable tool for tracking fluid behavior and ensuring process accuracy.

The antenna tag sensor design consists of two meandered strips in an S-shaped configuration. These strips are positioned symmetrically on either side of a centrally located ring resonator, ensuring balanced operation and effective impedance matching with the IC-chip. The circular ring resonator plays a crucial role in adjusting the resonant frequency of the antenna tag and serves as the connection point for the meandered strips. The chip is centrally mounted on the bottom of the ring resonator and communicates directly with the antenna to enable efficient signal transmission and reception. The entire structure is mounted on a flexible green polyimide substrate, known for its thin thickness, relative permittivity of 3.4, and loss factor 0.0025. The top layer of the antenna track is made of copper of the thickness of 35 µm. The overall size of the antenna structure is 49×39 mm, corresponding to $0.155\lambda \times 0.13\lambda$, where λ_0 is the free space wavelength at 915 MHz. This RFID tag sensor is designed to operate in the UHF RFID band of 868–928 MHz. The design utilizes NXP UCODE G2XL IC chip [17], which requires a minimum activation power of -18 dBm. In addition, the system is enhanced with a 3D printed PLA liquid channel integrated into the RFID tag antenna, forming a comprehensive sensor assembly which is shown in Figure 2. The final optimized geometric parameters were determined using Computer Simulation Technology (CST) Microwave Studio and are listed in Table 1.

The introduction of the ring into the RFID tag antenna serves to achieve a more compact design and to enhance interaction with the fluidic channel. Simulations show that a wider channel strengthens electric field interaction, thereby increasing sensitivity, while a narrower channel enhances field confinement, reducing interaction with the tag. These insights optimize performance for real-time liquid dielectric characterization.

TABLE 1. Dimensions of RFID tag antenna [mm].

Parameter	Dimension (mm)
W_{sub}	39
L_{sub}	49
W_a	19.20
W_b	24
L_a	34
L_b	3
R_1	9
R_2	9.5
g	2

To ensure optimal operation of this sensor in the reactive near field (RNF) of reading antenna, precise positioning of both the UHF antenna tag and reading antenna is required, for paramount importance is understanding the spatial extent of the RNF, which typically encompasses a region extending up to approximately one wavelength from the antenna surface [18]. To enable efficient power transfer and communication, UHF antenna tags must be strategically placed in this region to maximize proximity to the reading antenna without causing interference from nearby metallic or conductive objects. Careful adjustment of the distance between antennas is important to optimize coupling while avoiding saturation effects. Additionally, proper orientation to match polarization ensures maximum signal transmission efficiency. Rigorous testing validates the performance in the reactive near field and enables fine-tuning of antenna positioning for optimal RFID tag sensor functionality, for that the tag was positioned at a distance closer than the Fraunhofer distance from the antenna ($H_1 \ll H_f \sim 20\,\text{cm}$), as shown in Equation (1):

$$H_f = \frac{2 \times D^2}{\lambda} \tag{1}$$

Furthermore, λ symbolizes the wavelength of radiation at the operating frequency. This wavelength is vital in understanding the characteristics of the electromagnetic waves propagated by the antenna and their interaction with the surrounding environment. The interplay among H_f, D, and λ plays a pivotal role in determining the behavior and performance of the antenna system.

In addition to these factors, the distance between the tag and the antenna, called H_1, is important. For the sensor to work correctly, H_1 should be less than R, following the Fresnel region rules. By keeping this condition, the sensor operates within the reactive near field of the reader antenna. In this area, the electric field (E-Field) and magnetic field (H-Field) are 90 degrees out of sync with each other, as explained by Equation (2):

$$R = 0.62 \times \sqrt{\frac{D^3}{\lambda}} \tag{2}$$

The simulation results in Figure 3 show electric field across the RFID tag antenna at 915 MHz. The color gradient, from blue to red, indicates different field strengths, with red representing areas of higher intensity. These high-intensity regions are primarily located around the ring resonator and chip connection points, extending into the fluidic channel, emphasizing the role of these components in energy transfer and impedance matching. The strong fields around the resonator highlight its ability to concentrate electromagnetic energy, crucial for the antenna resonant behavior and operating frequency. The meandered S-shaped strips also show a balanced electric field distribution, indicating their role in fine-tuning the proposed antenna impedance and enhancing radiation efficiency. Additionally, the interaction of the electric field with a flexible polyimide substrate and fluidic channel underscores the importance of the liquid properties entering the channel in controlling field distribution and reducing losses. Overall, the simulation confirms that the antenna design is optimized for efficient energy confinement and effective radiation, ensuring strong performance within the UHF RFID band.

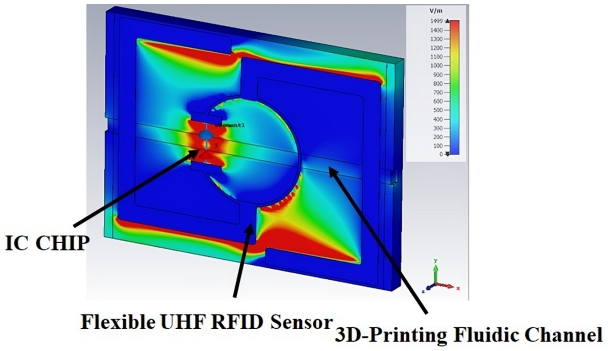

FIGURE 3. Electric field of the proposed RFID tag antenna.

From the simulation results, we can conclude that the absorption of electromagnetic waves in the reactive near-field region around the antenna is crucial for its reflection coefficient and input impedance. The reflection and impedance properties of the antenna are strongly influenced by how sensitive the near-field region is to electromagnetic absorption. The sensor detects changes in the electromagnetic field around a passive ring resonator when test materials are brought near it. The ring resonator creates areas of high or low electric field strength depending on how its gap is aligned with the antenna field. The gap in the ring, the most sensitive part of the label, responds significantly to changes in the permittivity or dielectric properties of the surrounding material.

Figure 4 illustrates the reflection coefficient as a function of frequency for various permittivity values ε_r of liquids in fluid channel positioned under proposed RFID tag antenna. The analysis shows a clear connection between the permittivity of the liquid and the resonance frequency of the antenna. As the permittivity increases from $\varepsilon_r = 5$ to $\varepsilon_r = 85$, a noticeable shift in the resonance frequency towards higher values is observed, moving from about 0.85 GHz to 1.02 GHz. This shift is attributed to the influence of the liquids permittivity on the effective dielectric constant of the antenna surroundings, with higher permittivity materials increasing the propagation delay of the electromagnetic wave, resulting in a shorter wavelength and consequently a higher resonance frequency. Furthermore,

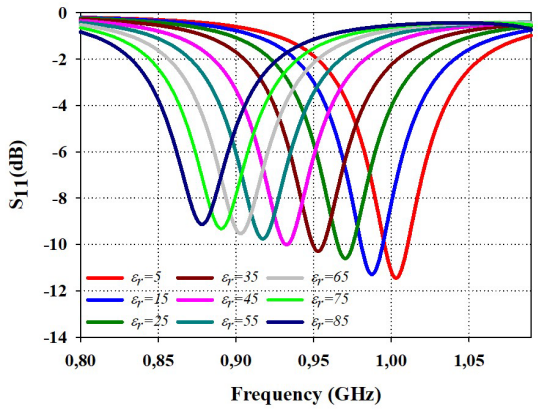

FIGURE 4. Reflection coefficient of the RFID tag antenna sensor with different dielectric constants into fluidic channel.

the minimum S_{11} values, which represent the point of maximum power transfer and minimum reflection, also vary slightly between different permittivity levels. In particular, higher permittivity led to deeper zeros, which suggests improved radiation efficiency at the corresponding resonance frequencies [22]. The spread of the S_{11} curves over a wider frequency range for higher dielectric constants indicates an expansion of the antenna operating bandwidth, allowing it to maintain efficient radiation over a wider frequency range. This behavior highlights the potential for fine-tuning the antenna performance by adjusting the permittivity of the liquid. The spread of the S_{11} curves over a wider frequency range for higher dielectric constants indicates an expansion of the antenna tag operating bandwidth, allowing it to maintain efficient radiation over a wider frequency range. This behavior highlights the potential for fine-tuning the antenna performance by adjusting the permittivity of the liquid in the fluid channel, making it possible to optimize the functionality of the antenna tag for specific UHF applications.

From these results we can demonstrate a clear mechanism by which the variation in the permittivity of liquids within a fluidic channel beneath a UHF antenna tag can be utilized as a sensing mechanism. As the permittivity of the liquid changes, there is a corresponding shift in antenna tag resonant frequency, moving from lower frequencies (around 0.85 GHz for $\varepsilon_r = 5$) to higher frequencies (approximately 1.02 GHz for $\varepsilon_r = 85$). This frequency shift is directly linked to the change in the dielectric properties of the environment surrounding the antenna, where higher permittivity values increase the effective dielectric constant, resulting in a shorter wavelength and a higher resonant frequency. The sensitivity of the resonant frequency to changes in permittivity suggests that this variation can be exploited for sensing applications. Specifically, by monitoring the resonant frequency shift, the antenna tag can effectively detect and quantify changes in the permittivity of the liquid in the channel, which may correspond to variations in the composition, concentration, or type of liquid being analyzed. This mechanism enables the antenna to function as a passive, wireless sensor, capable of providing real-time feedback on the properties of the liquid in the channel without the need for direct electrical contact. Such a sensing system could be highly valuable in applications such as chemical and biological sensing, environmental monitoring, and quality control, where detecting small changes in liquids properties is crucial. The tunable nature of the resonant frequency and the broad operational bandwidth further enhance the versatility and reliability of this sensing approach, making it a promising solution for a wide range of UHF sensing applications.

Figure 5 shows that both the real and imaginary parts of the antenna impedance are strongly influenced by the radius of the ring resonator (R_2) when the fluid channel is filled with deionized (DI) water. The real part, which corresponds to the resistance or radiation component, peaks at certain frequencies that shift depending on the antenna radius. Larger radii result in a peak at lower frequencies, while smaller radii shift the peak to higher frequencies, suggesting that the resonant frequency decreases as the antenna size increases. Similarly, the imaginary part of the impedance, which represents the reactive component, passes through zero at different frequencies and different R_2, indicating a transition between inductive and capacitive behaviors. This transition also occurs at larger R_2 at lower frequencies. These results highlight the importance of tuning the antenna radius to achieve the desired impedance characteristics and ensure that the antenna operates efficiently within the UHF frequency range. Proper tuning allows for better coordination between the antenna and RFID chip, thereby optimizing power transfer and the overall performance of the antenna.

The reflection coefficient results in Figure 6 show that parameter R_2 affects the resonance frequency and impedance matching of the antenna tag. As R_2 decreases from 2.8 mm to 1.4 mm, the resonance frequency shifts slightly higher, indicating that smaller radii push the resonance toward higher frequencies. Despite this shift, all configurations maintain a strong impedance match with an S_{11} value below -15 dB at resonance. Notably, the smallest radius of R_2 achieves better impedance matching at 881 MHz, indicating a slight improvement in performance. This ability to tune the resonant frequency by adjusting R_2 is important for optimizing the tag antenna performance in the UHF range, allowing for precise frequency alignment, efficient power transfer, and reduced reflection losses.

Impedance analysis for various gap parameters shows significant effects on both the real and imaginary components of the UHF antenna performance as shown in Figure 7. The real part of the impedance, which represents the resistance component, has clear resonance peaks that shift depending on the gap size. Larger gaps, such as 2.5 mm, produce resonance peaks at lower frequencies, while smaller dimension of the gaps, such as 0.8 mm, shift these peaks to higher frequencies, suggesting that the resonance frequency can be effectively controlled by adjusting the gap size. Furthermore, the amplitude of these peaks increases with larger gaps, suggesting improved radiation efficiency at certain frequencies. The imaginary part, which corresponds to the reactive part, also shows a strong dependence on the gap size, with transitions between inductive and capacitive behaviors occurring at frequencies that vary with the gap. Larger gaps lead to higher reactive magnitudes and lower transition frequencies, while smaller gaps lead these transitions to higher frequencies. These results highlight the crucial role of

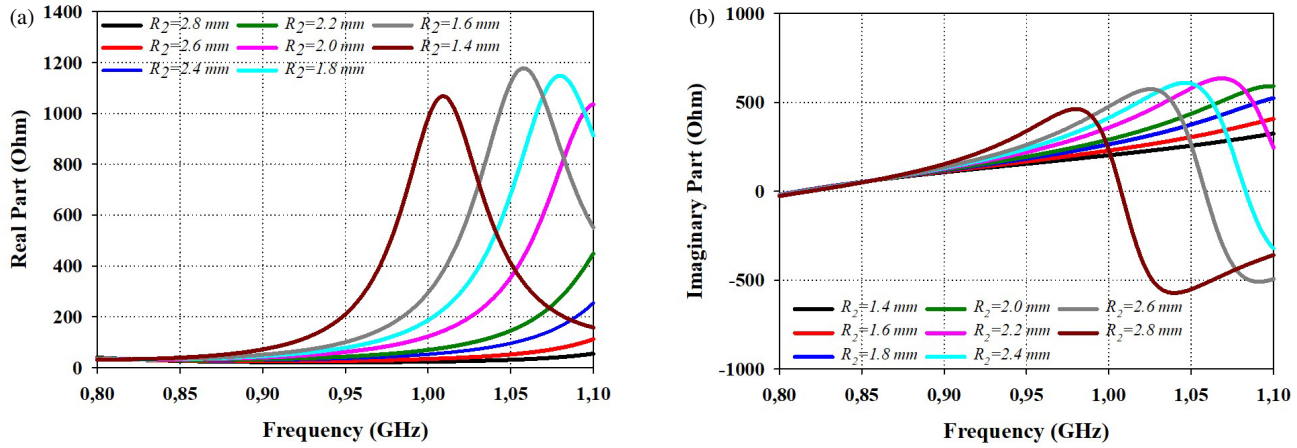

FIGURE 5. Simulated input impedance of the tag antenna sensor for various ring resonator gap R_2 values. (a) Real part; (b) Imaginary part.

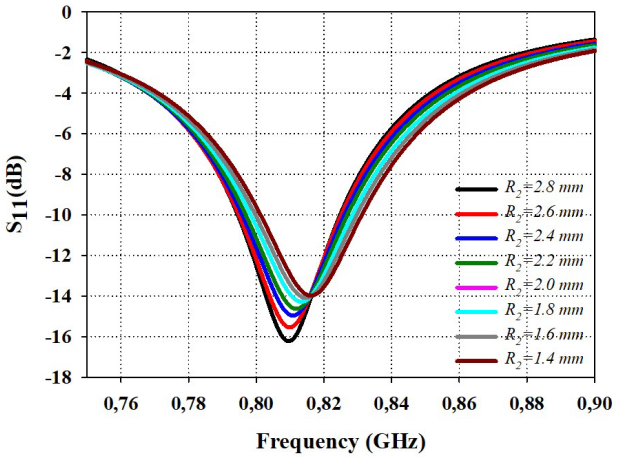

FIGURE 6. Simulated reflection coefficient of tag antenna sensor for different ring resonator values.

the mean gap parameter in tuning the antenna impedance and enable precise control of the resonant frequency and impedance characteristics.

The reflection coefficient as a function of frequency for different gap sizes of a UHF antenna tag is shown in Figure 8. The resonance frequency approximately 0.85 GHz remains constant across all gap sizes, indicating minimal frequency shift due to gap fluctuations. However, the gap size has a significant influence on the radiation efficiency of the antenna, as evidenced by the minimum S_{11} values. Smaller gaps, particularly 1.4 mm gap, have the lowest S_{11} values, indicating improved impedance matching and superior radiation efficiency. In contrast, larger gaps, such as the 2.8 mm gap, have higher power, suggesting poorer radiant performance. Additionally, the bandwidth, or frequency range, over which S_{11} remains below -10 dB is slightly wider for smaller gaps, suggesting that these configurations support more efficient radiation over a wider frequency range. These results show that optimizing the gap size, particularly towards smaller dimensions, is crucial for maximizing the performance of UHF antenna tags, both in terms of radiation efficiency and operating bandwidth.

3. MEASUREMENT RESULTS AND DISCUSSIONS

To validate the results, a prototype of the proposed RFID tag antenna sensor was fabricated and tested, and 3D-fluidic channel is also fabricated using 3D printing technology for this purpose. The channel is constructed from PLA material with a permittivity of 2.1 and a loss factor of 0.02 [19]. 1.5 mm in width, 30 mm in length of the liquid, and 500 µm in height provide a capacity of 2.3 milliliters. This is illustrated in Figure 9, and the microfluidic channel is securely bonded to the passive RFID tag, ensuring stability and minimizing mechanical noise or drift. Standard liquids, including water, acetic acid, and ethanol, are introduced into the liquids channel using a syringe pump, visible on either side of the setup, maintaining a constant flow rate of 1 mL/min for consistent liquid flow. The RFID tag, attached to the fluidic channel, is centrally positioned between absorber foams, at a distance of 15 cm from the absorber walls. This arrangement is crucial for obtaining accurate and controlled measurements during the liquid characterization process, as it effectively isolates the tag from external electromagnetic interference. A ruler placed beneath the tag provides a scale reference, highlighting the compactness of the setup.

The tag antenna reflection scattering parameter was measured using a Keysight vector network analyzer (VNA), as shown in Figure 10. The measured data was used to calculate the reflection coefficient. The VNA was set up with a bandwidth of 300 Hz and an output power of 10 dBm and collected a total of 3601 data points. These settings enabled accurate measurement and analysis of the antenna performance and its response to the RFID tag.

In this study, the experimental setup designed to measure the resonant frequency of various liquids using the proposed RFID sensor antenna is shown in Figure 10(a). We use port extension technique to measure the power reflection coefficient, and this technique is detailed in [20]. The antenna is connected to a coaxial cable that interfaces with the measurement equipment. To begin the experiment, the RFID sensor tag is connected to a Vector Network Analyzer (VNA), as shown in Figure 10(b). The VNA is calibrated to ensure accurate measurements across the desired frequency range, typically covering the UHF RFID

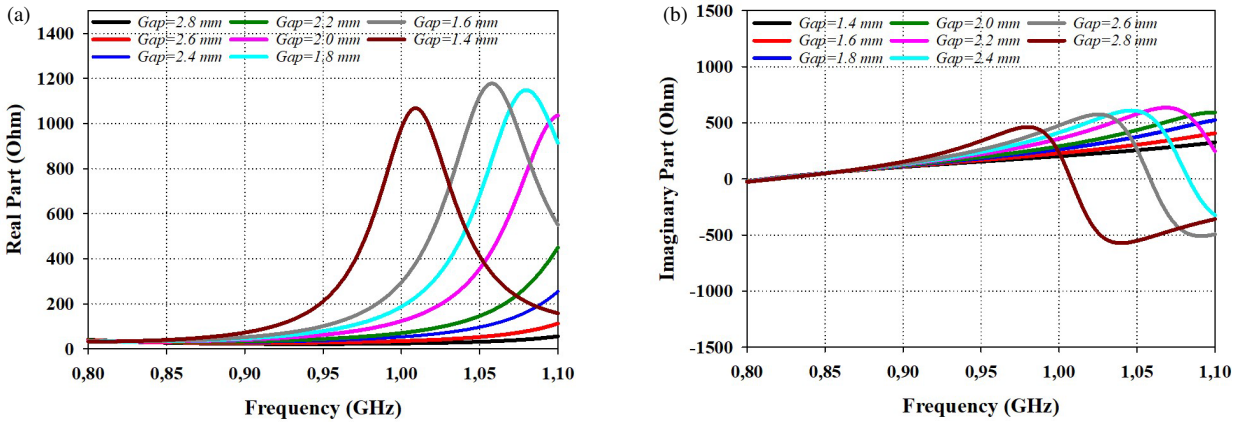

FIGURE 7. Simulated input impedance of the tag antenna sensor for different gap values. (a) Real part; (b) Imaginary part.

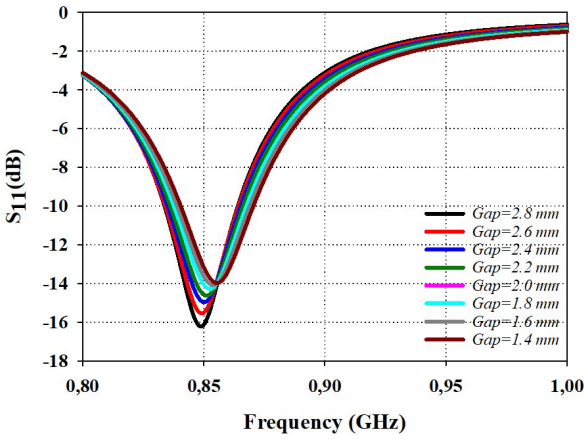

FIGURE 8. Simulated reflection coefficient of tag antenna sensor for different gap sizes.

band (902–928 MHz). Once calibration is complete, the VNA is used to measure the reflection coefficient of the RFID sensor antenna in different environments, specifically with various liquids. The liquids are introduced into the system through a pump, which can be seen in the foreground of Figure 9(b). The pump is connected to the RFID sensor via channel, allowing controlled amounts of liquid to flow through the integrated fluid channel of the antenna. Common test liquids include water, acetic acid, ethanol, 5% glucose, each of which has distinct permittivity values. As the liquid passes through the channel, the interaction between the liquid and electromagnetic fields of the antenna alters the resonance characteristics of the sensor. The VNA records the reflection coefficient for each liquid, and these measurements are analyzed to determine the effective permittivity of the liquid. This analysis is based on the shift in the resonance frequency of the antenna, which is sensitive to changes in the dielectric environment. The results provide valuable information on the dielectric properties of the test liquids, which can be used for various sensing applications. This setup highlights the use of RFID technology in sensing applications, where the flexible nature of the antenna and its integration with 3D-fluidic channel enable real-time monitoring of the permittivity of liquids. By treating the antenna as a two-port network and measuring the associated S-parameters, the

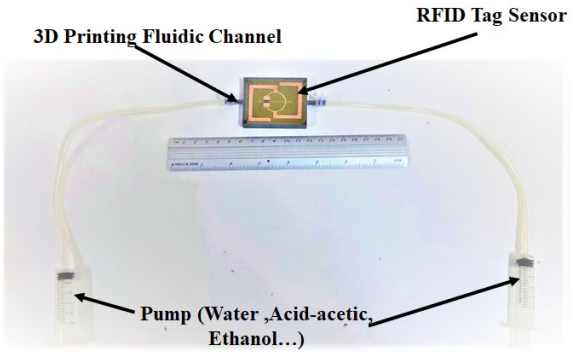

FIGURE 9. Prototype of the RFID tag sensor with a 3D fluid channel.

input impedance of the tag antenna, Z_{in} can be calculated from equation

$$Z_{in(ant)} = \frac{2Z_0\left(1 - S_{11}^2 + S_{21}^2 - 2S_{12}\right)}{\left(1 - S_{11}\right)^2 - S_{21}^2} \tag{3}$$

Then

$$S_{11} = \frac{Z_{in(ant)} - Z_{chip}}{Z_{in(ant)} + Z_{chip}} \tag{4}$$

The results obtained from the experimental technique are shown in Figure 11, which shows the reflection coefficient as a function of frequency for the flexible RFID sensor tag when it is exposed to various liquids including ethyl alcohol, acetic acid, 5% of the glucose, ethanol, and DI water as well as an empty condition for baseline comparison. S_{11} is critical because it quantifies the amount of power reflected by the sensor, with lower S_{11} values indicating stronger interactions between the sensor and liquid medium. The results clearly show that each liquid induces a significant resonance dip in the reflection coefficient, with this variation occurring at different frequencies depending on the permittivity of the liquid. The empty state has a resonance around 1 GHz, which serves as a reference point. However, when different liquids are introduced, significant shifts in the resonance frequency are observed. DI water, represented by the black curve, causes a significant shift to a lower frequency, reflecting its higher permittivity than the

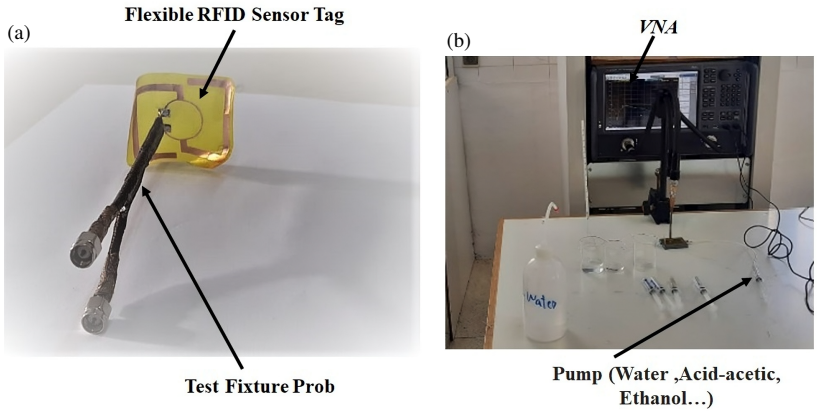

FIGURE 10. Setup for impedance measurement of the proposed tag antenna. (a) Test fixture probe; (b) Experimental setup.

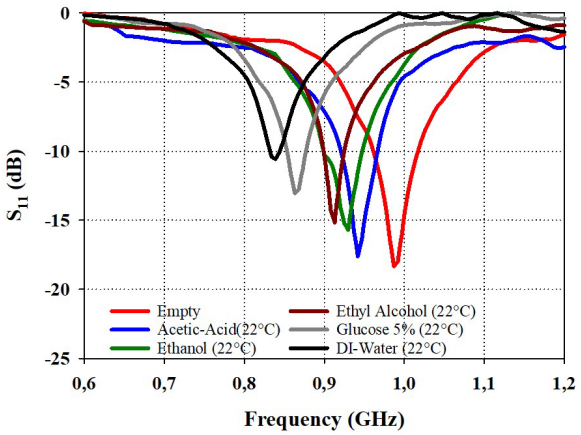

FIGURE 11. Measured power reflection coefficient of the tag antenna sensor for various liquids.

other liquids tested. Conversely, ethyl alcohol, represented by the brown curve, results in a resonance at a higher frequency, indicating its lower permittivity. The depth and location of these resonance dips are directly related to the dielectric properties of the respective liquids, confirming the sensor ability to distinguish substances based on their permittivity.

The ability of the proposed RFID tag antenna sensor to distinguish between different liquids is largely determined by the interaction between the electromagnetic field generated by the sensor and the dielectric properties of the surrounding medium. When the flexible RFID sensor tag is connected to a Vector Network Analyzer (VNA), it emits an RF signal that propagates through the sensor and interacts with the adjacent liquid. The dielectric permittivity of the liquid, which quantifies the liquids capacity to store electric field energy, has a direct impact on the RFID antenna sensor impedance. This interaction influences the reflection coefficient, represented by the S_{11} parameter, which is measured by the VNA. Variations in the liquid permittivity alter the distribution of the electric field within the sensor, resulting in shifts in the resonance frequency and variations in the depth of the resonance dips observed in the S_{11} versus frequency. For example, liquids with higher permittivity, such as DI-water, cause a downward shift in the resonance frequency, indicating a stronger interaction with the sensor electromagnetic field. On the other hand, liquids with lower permittivity, such as ethyl alcohol, result in an upward shift in the resonance frequency, reflecting a weaker interaction. This relationship is essential to the sensor functionality, as it enables the RFID sensor tag to effectively sense and distinguish between liquids based on their unique dielectric properties.

4. OPERATING PRINCIPLE OF THE RFID TAG ANTENNA AS A SENSOR AND ITS WORKING MECHANISM

The working principle of the system is based on the utilization of RFID technology to detect and differentiate liquids. In this approach, we have a liquid sample under investigation introduced into a fluidic channel with a specific solution, which is carefully chosen based on the desired testing parameters. An RFID tag antenna is then immersed in this liquid-filled channel. The tag sensor is subsequently positioned near an RFID reader to ensure that the tag can communicate effectively through backscatter modulation, a technique where the tag reflects a portion of the reader signal back with modulated data as shown in Figure 12.

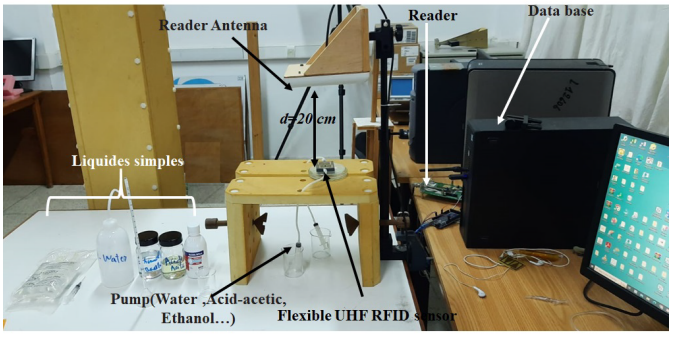

FIGURE 12. Photograph of the experimental setup for liquid detection.

The sensitivity of the RFID-UHF tag antenna, which is crucial for accurate liquid detection, can be quantitatively described by the following equation [4]:

$$S_{tag} = P_{tx,ON} \cdot G_{tx} \cdot \tau \cdot \left(\frac{\lambda}{4\pi d}\right)^2 \cdot \eta_{plf} \cdot A_{cable} \qquad (5)$$

In this equation, G_{tx} represents the gain of the RFID reader antenna, a measure of how effectively it can transmit and receive signals. The term η_{plf} denotes the polarization mismatch between the RFID reader antenna and the tag, which can affect the efficiency of communication. The transmission coefficient τ of the RFID tag reflects how much of the incoming RF signal is transmitted through the tag circuitry. A_{cable} accounts for any signal attenuation that may occur in the cables connecting the RFID system components. $P_{tx,ON}$ represents the transmitted power when the RFID reader is actively sending signals. The actual amount of power that is transferred from the RFID antenna to the chip embedded within the tag is influenced by the interaction or coupling between them. This coupling is critical as it determines how effectively the tag can process and reflect the signal back to the reader. The power that is successfully coupled to the chip is described by:

$$S_{chip} = \left(1 - |\Gamma_{tag}|^2\right) \cdot G_{tag} \cdot S_{tag} \tag{6}$$

Here, Γ_{tag} represents the reflection coefficient at the tag antenna, a key factor that depends on the impedance matching between the antenna and its surrounding environment. G_{tag} is the gain of the tag antenna, influencing how well the tag can transmit the backscattered signal. When irrelevant parameters are simplified and excluded, the relationship is simplified to:

$$S_{tag} \propto \frac{1}{\left(1 - |\Gamma_{tag}|^2\right) \cdot G_{tag}} \tag{7}$$

The experimental steps began with the assembly and calibration of the RFID measurement system, which included a ThingMagic RFID reader equipped with a circular polarization reader antenna [21] shown in Figure 12. The antenna was strategically positioned about 20 cm above the sensor to maintain consistent signal transmission. A variety of liquid samples, such as water, acetic acid, ethanol, ethyl alcohol, 5% of glucose, were prepared and introduced beneath the sensor using a calibrated peristaltic pump to ensure precise volume and uniform coverage. For each liquid, the sensor response, including the sensitivity of the tag (S_{tag}) and any potential frequency shifts, was recorded by the reader and logged into a computer system for further analysis. To ensure accuracy and reliability, each measurement was repeated five times. The data collected was then compared to a baseline measurement taken in air, enabling an assessment of the RFID sensor sensitivity to the different liquid samples. Statistical analysis was conducted to quantify the repeatability of the measurements and to evaluate the sensor performance in detecting variations in the liquid dielectric properties.

Figure 13 presents a comprehensive analysis of how the sensitivity of the RFID tag sensor changes with frequency when it was exposed to different liquid samples at 22°C. Over the frequency range of 0.865 GHz to 0.869 GHz, the sensor consistently displayed high sensitivity values in the empty state, ranging from 2.1 dBm to 3.5 dBm, which is well above the sensitivity threshold of the IC-chip. However, there is an interaction effect present even without liquids. Both acetic acid and ethanol showed nearly constant Stag values around 0.1 dBm

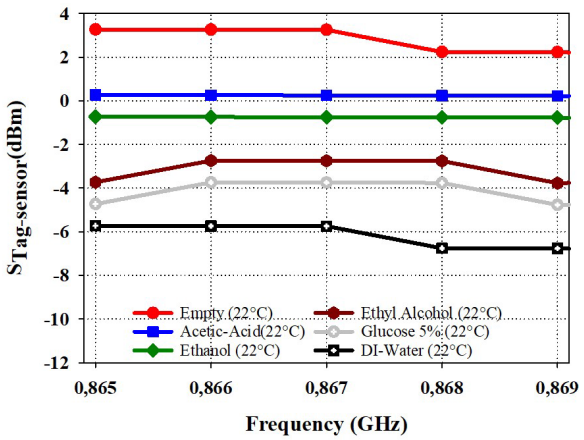

FIGURE 13. Sensitivity of the RFID tag sensor varies with different liquid solutions at various frequencies.

and -0.5 dBm at 0.865 GHz, respectively. Upon exposure to ethyl alcohol, the Stag value decreases slightly from approximately -4 dBm at 0.865 GHz, reflecting minimal frequency sensitivity. In contrast, the 5% glucose solution exhibited a gradual decrease in Stag to -5 dBm at 0.865 GHz, indicating a moderate effect on signal strength that becomes more apparent at higher frequencies. The most pronounced frequency-dependent behavior was observed with deionized (DI) water, where the Stag values decreased to -7 dBm at 0.868 GHz, which is closer to the sensitivity threshold of the IC chip. This significant decrease highlights the strong interaction of water with the RFID signal, which is due to its high dielectric constant and results in decreased signal absorption and attenuation, especially at higher frequencies.

5. CONCLUSION

In this study, we present a novel RFID-UHF tag antenna sensor designed for the detection and differentiation of liquids based on their dielectric properties. The sensor, integrated with a fluidic channel, operates within the 865–869 MHz RFID-UHF band and utilizes backscatter modulation for communication with a nearby RFID reader. Experimental results demonstrate the proposed sensor ability to distinguish among various liquids, including water, ethanol, acetic acid, and glucose solution, by analyzing frequency-dependent changes in the tag sensitivity (S_{tag}). Notably, deionized water exhibited the most significant interaction, with S_{tag} values decreasing sharply across the frequency range due to its high dielectric constant, which led to increased signal absorption and attenuation. This frequency-dependent behavior underscores the potential of the proposed RFID sensor for applications requiring precise liquid identification and monitoring, offering a robust, noninvasive solution for real-time analysis in diverse fields such as chemical processing, biomedical diagnostics, and environmental sensing.

REFERENCES

[1] Kim, D.-H., N. Lu, R. Ma, Y.-S. Kim, R.-H. Kim, S. Wang, J. Wu, S. M. Won, H. Tao, A. Islam, *et al.*, "Epidermal electronics," *Science*, Vol. 333, No. 6044, 838–843, Aug. 2011.

[2] Dobkin, D., *The RF in RFID: Passive UHF RFID in Practice*, 2nd ed., Elsevier, Amsterdam, The Netherlands, 2013.

[3] Ali, M. K. and T. Rahman, "Wireless RFID sensing for IoT applications," *IEEE Sensors Journal*, Vol. 18, No. 4, 1234–1241, Feb. 2018.

[4] Ennasar, M. A., O. E. Mrabet, K. Mohamed, and M. Essaaidi, "Design and characterization of a broadband flexible polyimide RFID tag sensor for NaCl and sugar detection," *Progress In Electromagnetics Research C*, Vol. 94, 273–283, 2019.

[5] Wiltshire, B. D., T. Zarifi, and M. H. Zarifi, "Passive split ring resonator tag configuration for RFID-based wireless permittivity sensing," *IEEE Sensors Journal*, Vol. 20, No. 4, 1904–1911, Feb. 2020.

[6] Vélez, P., K. Grenier, J. Mata-Contreras, D. Dubuc, and F. Martin, "Highly-sensitive microwave sensors based on open complementary split ring resonators (OCSRRs) for dielectric characterization and solute concentration measurement in liquids," *IEEE Access*, Vol. 6, 48 324–48 338, 2018.

[7] Seo, Y., M. U. Memon, and S. Lim, "Microfluidic eighth-mode substrate-integrated-waveguide antenna for compact ethanol chemical sensor application," *IEEE Transactions on Antennas and Propagation*, Vol. 64, No. 7, 3218–3222, Jul. 2016.

[8] Virtanen, J., *et al.*, "Wireless liquid sensing with dual-resonant UHF RFID tags," *IEEE Transactions on Microwave Theory and Techniques*, Vol. 60, No. 7, 2305–2313, Jul. 2012.

[9] Bianco, G. M. and G. Marrocco, "Joint design of self-tuning UHF RFID antenna and microfluidic channel for liquid sensing," *IEEE Journal of Radio Frequency Identification*, Vol. 8, 58–67, Apr. 2024.

[10] Bhattacharyya, R., F. V. Gonzalez, and P. Nikitin, "Material sensing using RAIN RFID tags with auto-tuning capabilities," *IEEE Journal of Radio Frequency Identification*, Vol. 9, 340–349, May 2025.

[11] Rida, A., M. Tentzeris, and L. Yang, *RFID-Enabled Sensor Design and Applications*, Artech, 2010.

[12] Tentzeris, M. and A. Rida, "Inkjet-printed RFID-enabled sensors: Towards real-world applications," *IEEE Proceedings*, Vol. 105, No. 1, 104–116, Jan. 2017.

[13] Mohamadzade, B., R. B. V. B. Simorangkir, S. Maric, A. Lalbakhsh, K. P. Esselle, and R. M. Hashmi, "Recent developments and state of the art in flexible and conformal reconfigurable antennas," *Electronics*, Vol. 9, No. 9, 1375, Sep. 2020.

[14] Zhang, J., G. Y. Tian, A. M. J. Marindra, A. I. Sunny, and A. B. Zhao, "A review of passive RFID tag antenna-based sensors and systems for structural health monitoring applications," *Sensors*, Vol. 17, No. 2, 265, Feb. 2017.

[15] Ren, Y. J. and K. Chang, "Microfluidics-based reconfigurable liquid dielectric antenna," *IEEE Transactions on Antennas and Propagation*, Vol. 60, No. 2, 773–780, Feb. 2012.

[16] Kim, K. S., *et al.*, "Flexible RFID tag antenna for liquid sensing," *IEEE Transactions on Antennas and Propagation*, Vol. 61, No. 1, 483–487, Jan. 2013.

[17] https://www.nxp.com/products/rfid-nfc/ucode-rain-rfid-uhf/ucode-g2il-and-g2il-plus:SL3S1203_1213.

[18] Salim, A. and S. Lim, "Review of recent metamaterial microfluidic sensors," *Sensors*, Vol. 18, No. 1, 232, Jan. 2018.

[19] Huber, E., M. Mirzaee, J. Bjorgaard, M. Hoyack, S. Noghanian, and I. Chang, "Dielectric property measurement of PLA," in *2016 IEEE International Conference on Electro Information Technology (EIT)*, 0788–0792, Grand Forks, ND, USA, May 2016.

[20] El Khamlichi, M., A. A. Melcon, O. E. Mrabet, M. A. Ennasar, and J. Hinojosa, "Flexible UHF RFID tag for blood tubes monitoring," *Sensors*, Vol. 19, No. 22, 4903, 2019.

[21] Ennasar, M. A., I. Aznabet, O. E. Mrabet, and M. Essaaidi, "Design and characterization of a compact single layer modified S-shaped tag antenna for UHF-RFID applications," *Advanced Electromagnetics*, Vol. 8, No. 1, 59–65, 2019.

[22] Liu, Y., T. Dong, X. Qin, W. Luo, N. Leng, Y. He, Y. Yuan, M. Bai, J. Sun, J. Zhou, *et al.*, "High-permittivity ceramics enabled highly homogeneous zero-index metamaterials for high-directivity antennas and beyond," *Elight*, Vol. 4, No. 1, 4, 2024.